[2] Slomyanski, G. A. and Pryadilov, U. N., *Floated Gyroscopes and Their Application* (Oborongiz, State Defense Press, 1958).
[3] Collinson, R. P. G., "Inertial navigation, 1960," Flight no. 2658, 19/II (1960).
[4] Murphy, G. J., *Basic Automatic Control Theory* (New York, 1957).
[5] Olman, E. V., Solovev, Y. I., and Tokarev, V. P., *Autopilot* (Oborongiz, State Defense Press, 1946).
[6] Braslavski, D. A., Logonov, S. S., and Pelpor, D. C., *Design and Construction of Aviation Instruments* (Oborongiz, State Defense Press, 1954).
[7] Litvin-Sedoy, M. Z., "The geometry of gyroscopic angular position measuring instruments," University Repts., Physical-Mathematical Science, no. 3 (1958).
[8] Litvin-Sedoy, M. Z., "Determination of the angular position of a body with the aid of gyroscopic accelerometers which have arbitrary inclinations of their case axes in a body moving in space," *Mechanics, MVTU* (*Moscow Technical College*), edited by N. E. Bauman (Oborongiz, State Defense Press, 1959).
[9] Litvin-Sedoy, M. Z., "Some geometric relationships in mechanical systems with many degrees of freedom," Bul. Inst. Politehnic Iasi, serie noua **IV**, no. 8, 1–2 (1958).
[10] Dvlone, B. N. and Raykov, D. A., *Analytical Geometry* (GTTI, State Technical Press, 1948).

Reviewer's Comment

The basic objective of this paper is exactly as specified by its title and is succinctly executed, although the notation employed could easily be improved. The problem is a straightforward exercise in linear matrix algebra and transformations between non-orthogonal coordinate systems. Because the usual courses in vector and matrix algebra usually slight this problem and the relationships between parallel and perpendicular projections in such a coordinate system, it should prove interesting for the reader to deduce for himself the stated results [specifically Eqs. (1–5) of the paper].

The results themselves are well known and have been derived and widely used, for example, in the error analysis of attitude-control systems (see, e.g., Ref. 1) and inertial navigation systems. In the latter type of system it is customary, though not mandatory, to place the accelerometers and gyros so that their sensitive axes are aligned along the (orthogonal) navigation axes. Thus any deviations are assumed small, so that small-angle approximations are applicable and the error analysis is considerably simplified, the transformation matrices being then of a very simple nature (see, e.g., Ref. 2).

—CARLETON B. SOLLOWAY
Jet Propulsion Laboratory
California Institute of Technology

[1] Roberson, R. E., "A unified analytical description of satellite attitude motions," ARS Preprint 722–58 (1958).
[2] Savant, C. J. et al., *Principles of Inertial Navigation* (McGraw-Hill Book Company, Inc., New York, 1961), Chap. 10.

SEPTEMBER 1963 AIAA JOURNAL VOL. 1, NO. 9

Numerical Solution of the Problem of Supersonic Flow past the Lower Surface of a Delta Wing

D. A. BABAEV

WHEN supersonic flow takes place past a plane delta wing, there is a shock wave upstream of the lower surface. We shall consider cases in which this shock wave is attached to the leading edges of the wing. In this case the flow past the wing will be conical (with center of conicity at the apex of the wing), and the flows past the upper and lower surfaces will be independent. The flow past the upper surface of the wing was investigated in Ref. 1. In the present study we shall solve the problem of flow past the lower surface.

In conical flow all the variables which characterize the flow are constant along lines radiating from a center of conicity. We shall adopt a rectangular system of coordinates associated with the wing, as follows: the origin is at the apex of the wing, at the center of conicity; the Ox axis is directed along the root chord from the apex of the wing toward the trailing edge; the Oy axis is in the plane of the wing, directed toward the right half-wing; the Oz axis is perpendicular to the plane of the wing, directed toward the lower surface.

The position of a straight line emanating from the apex of the wing is determined by the quantities $\eta = y/x$, $\xi = z/x$; thus, all of the flow parameters will be functions of the two variables η and ξ, which may be considered as dimensionless conical coordinates. The (η,ξ) plane corresponds to the physical plane $x = 1$ perpendicular to the root chord of the wing.

We introduce the entropy function

$$\tilde{s} = \frac{1}{\varkappa(\varkappa - 1)} \ln \frac{P/P_\infty}{(\rho/\rho_\infty)^\varkappa}$$

$$u = v_x/V_\infty \qquad v = v_y/V_\infty \qquad w = v_z/V_\infty$$

$$\tilde{a} = a/V_\infty \qquad U^2 = u^2 + v^2 + w^2$$

Here v_x, v_y, and v_z are the velocity components along the coordinate axes, V_∞ the velocity of the oncoming flow, a the

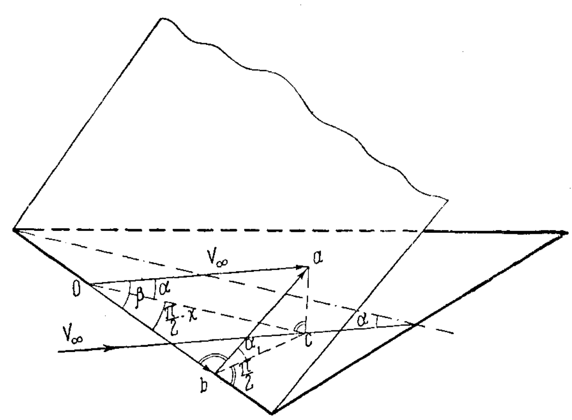

Fig. 1.

Translated from Zhurnal Vychislitel'noi Matematiki i Matematicheskoi Fiziki (Journal of Computational Mathematics and Mathematical Physics) **2**, No. 6, 1086–1101 (November–December 1962). Translated by Alexander Schwartz, New York.

velocity of sound, P the pressure, ρ the density, and κ the specific heat ratio. Then the equations of motion and continuity may be written in the form

$$v\left(\eta \frac{\partial v}{\partial \eta} + \xi \frac{\partial v}{\partial \xi} + \frac{\partial u}{\partial \eta}\right) + w\left(\eta \frac{\partial w}{\partial \eta} + \xi \frac{\partial w}{\partial \xi} + \frac{\partial u}{\partial \xi}\right) = -\tilde{a}^2\left(\eta \frac{\partial \tilde{s}}{\partial \eta} + \xi \frac{\partial \tilde{s}}{\partial \xi}\right)$$

$$u\left(\eta \frac{\partial v}{\partial \eta} + \xi \frac{\partial v}{\partial \xi} + \frac{\partial u}{\partial \eta}\right) + w\left(\frac{\partial w}{\partial \eta} - \frac{\partial v}{\partial \xi}\right) = -a^2 \frac{\partial \tilde{s}}{\partial \eta} \quad (1)$$

$$u\left(\eta \frac{\partial w}{\partial \eta} + \xi \frac{\partial w}{\partial \xi} + \frac{\partial u}{\partial \eta}\right) + v\left(\frac{\partial v}{\partial \xi} - \frac{\partial w}{\partial \eta}\right) = -\tilde{a}^2 \frac{\partial \tilde{s}}{\partial \xi}$$

$$2\tilde{a}^2\left(\eta \frac{\partial u}{\partial \eta} + \xi \frac{\partial u}{\partial \xi} - \frac{\partial v}{\partial \eta} - \frac{\partial w}{\partial \xi}\right) + (v - u\eta)\frac{\partial U^2}{\partial \eta} + (w - u\xi)\frac{\partial U^2}{\partial \xi} = 0$$

At the leading edge of the wing the shock wave must satisfy the relations

$$V_{n\infty} \cdot V_n = a_*^2 - \frac{\kappa - 1}{\kappa + 1} V_t^2 \quad (2a)$$

$$V_{t\infty} = V_t \quad (2b)$$

Here $V_{n\infty}$ and V_n, $V_{t\infty}$, and V_t are the velocity components respectively normal and tangent to the surface of the shock wave, before and behind it, respectively, and a_* is the critical velocity of sound.

We introduce the following notation: α_1 is the angle between the plane of the wing and the plane passing through the leading edge parallel to the velocity of undisturbed flow, ϵ the angle between this last plane and the plane of the shock wave; and β the angle between the direction of the velocity of undisturbed flow and the leading edge.

From geometrical considerations we can obtain (see Fig. 1):

$$\alpha_1 = \arctan(\tan\alpha/\cos\chi) \quad (3)$$

$$\beta = \arccos(\cos\alpha \cdot \sin\chi)$$

$$V_{n\infty} = V_\infty \sin\beta \sin\epsilon$$

$$V_{t\infty}^2 = V_\infty^2(1 - \sin^2\beta \sin^2\epsilon) \quad (4)$$

Here χ is the sweepback angle of the wing at the leading edge, and α is the angle of attack.

Taking Eq. (2b) into consideration, we find

$$V_n = V_{n\infty} \sin\beta \cos\epsilon \tan(\epsilon - \alpha_1) \quad (5)$$

Substituting Eqs. (4) and (5) into (2b), after some transformations, we obtain

$$\left(1 + \frac{\kappa - 1}{2} M_\infty^2 \sin^2\beta\right)\tan^3\epsilon - (M_\infty^2 \sin^2\beta - 1)\,\mathrm{cotan}\,\alpha_1 \tan^2\epsilon + \left(1 + \frac{\kappa + 1}{x} M_\infty^2 \sin^2\beta\right)\tan\epsilon + \mathrm{cotan}\,\alpha_1 = 0 \quad (6)$$

For known values of M_∞, α, and χ, this equation determines the angle of inclination ϵ of the shock. A similar equation for the oblique shock in two-dimensional flow can be written

$$\left(1 + \frac{\kappa - 1}{2} M_\infty^2\right)\tan^3\epsilon_{pl} - (M_\infty^2 - 1)\,\mathrm{cotan}\,\alpha_{pl} \tan^2\epsilon_{pl} + \left(1 + \frac{\kappa + 1}{2} M_\infty^2\right)\tan\epsilon_{pl} + \mathrm{cotan}\,\alpha_{pl} = 0 \quad (7)$$

Here ϵ_{pl} is the angle between the plane of the shock and the undisturbed velocity, whereas α_{pl} is the angle of deflection of the flow by the oblique shock.

Fig. 2.

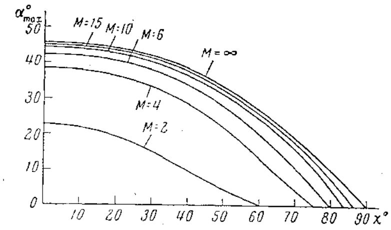

The quantities $M_\infty \sin\beta$, ϵ, and α_1 in Eq. (6) are, respectively, M_∞, ϵ_{pl}, and α_{pl} in a plane perpendicular to the leading edge of the wing. Thus, Eq. (6) is a generalization of the equation of an oblique shock (7) for the case of a sliding wedge.

If the value of ϵ is known, then the velocity components behind the shock wave near the leading edge of the delta wing are determined by*

$$u = \cos\beta \sin\chi + \frac{\sin\beta \cos\epsilon \cos\chi}{\cos(\epsilon - \alpha_1)}$$

$$v = \cos\beta \cos\chi - \frac{\sin\beta \cos\epsilon \sin\chi}{\cos(\epsilon - \alpha_1)} \quad (8)$$

$$w = 0$$

The change of entropy in passing through the shock is calculated by

$$\Delta\tilde{s} = \tilde{s} - \tilde{s}_\infty = \frac{1}{\kappa(\kappa - 1)} \ln\left[\frac{2\kappa}{\kappa + 1}\left(M_\infty^2 \sin^2\beta \sin^2\epsilon - \frac{\kappa - 1}{2\kappa}\right)\right] + \frac{1}{\kappa - 1} \ln\left[\frac{2}{\kappa + 1}\left(\frac{1}{M_\infty^2 \sin^2\beta \sin^2\epsilon} + \frac{\kappa - 1}{2}\right)\right] \quad (9)$$

The maximum value of ϵ, for which a shock wave attached to the leading edge is possible, is determined by

$$\sin\epsilon_{\max} = \frac{1}{\kappa M_\infty^2 \sin^2\beta}\left[\frac{\kappa + 1}{4} M_\infty^2 \sin^2\beta - 1 + \sqrt{(\kappa + 1)\left(1 + \frac{\kappa + 1}{2} M_\infty^2 \sin^2\beta + \frac{\kappa + 1}{16} M_\infty^2 \sin^2\beta\right)}\right] \quad (10)$$

Formula (10) is obtained from the corresponding relations for two-dimensional flow by replacing M_∞ by $M_\infty \sin\beta$. Eliminating ϵ, we can use (10) and (6) to determine the maximum values of the angle of attack $\alpha_{\max} = f(M_\infty, \chi)$ that permits independent flow past the two wing surfaces. These values of $\alpha_{\max}$ mark the boundaries of the region in which the methods of the present study are applicable (Fig. 2).

1. Statement of the Problem for the Region of Influence of the Apex of the Wing

On the side of the lower surface of the wing, uniform flow with velocity components (8) exists near the leading edge A (Fig. 3) between the shock wave AB, whose equation is of the form

$$\xi = \tan(\epsilon - \alpha_1) \sin\chi(\cot\chi - \eta) \quad (11)$$

and the wing surface AO. The region of uniform flow is bounded by the Mach cone BD corresponding to this flow according to the relation

$$Q(1 + \eta^2 + \xi^2) = (u + \eta v + \xi w)^2 \quad (12)$$

where

$$Q = \frac{\kappa + 1}{2} U^2 - \frac{1}{M_\infty^2}\left(1 + \frac{\kappa - 1}{2} M_\infty^2\right)$$

* The expression for v is written for the right half-wing.

In the central region of the wing the flow is determined by the mutual influence of the two halves of the wing. At the point B, the point of intersection of the Mach cone BD and the shock wave AB, the latter begins to curve:

$$\eta_B = \frac{b + \sqrt{b^2 - ac}}{a} \tag{13}$$

$$\xi_B = \tan(\epsilon - \alpha_1)(\cos\chi - \eta_B \sin\chi)$$

where

$$a = Q[1 + \sin^2\chi \tan^2(\epsilon - \alpha_1)] - v^2$$

$$b = Q \sin\chi \cos\chi + uv$$

$$c = Q[1 + \cos^2\chi \tan^2(\epsilon - \alpha_1)] - u^2$$

The strength of the shock is reduced between point B and the plane of symmetry of the wing. The velocity components behind the conical density jump are determined by the following equations:

$$u_c = u - \left(\frac{f}{f'} - \eta\right)f' \cdot R \qquad v_c = v - f' \cdot R$$

$$w_c = w + R \tag{14}$$

Here u, v, and w are the velocity components in front of the shock; in particular, in front of BC:

$$u = \cos\alpha \qquad v = 0 \qquad w = -\sin\alpha$$

Here $f = f(\eta)$ is the equation of the shock wave, $f' = df/d\eta$:

$$R = \frac{2}{\varkappa + 1}\left[\frac{\omega_1}{\omega_2} + \frac{1}{\omega_1}(Q - U^2)\right]$$

where

$$\omega_1 = (f - \eta f')u + f'v - w$$

$$\omega_2 = 1 + (f - \eta f')^2 + f'^2$$

The change in entropy in passing through the shock wave is determined from formula (9), where instead of $M_\infty^2 \sin^2\beta \sin^2\epsilon$ we must substitute $M_\infty^2(\omega_1^2/\omega_2)$.

The shock wave ABC bounds the region of flow disturbed by the presence of the wing on the side of the lower surface. Between point B and the plane of symmetry of the wing ($\eta = 0$) the shape of the shock wave BC is unknown and must be determined. The following facts are known about the shape of BC, that is, $f = f(\eta)$:

1) BC is tangent to AB at the point B:

$$\left(\frac{df}{d\eta}\right)_B = -\tan(\epsilon - \alpha_1) \cdot \sin\chi$$

$$\left(\frac{df}{d\eta}\right)_{\eta=0} = 0 \tag{15}$$

The latter condition results from the second equation of (14) if we consider that $v_c = v = 0$ for $\eta = 0$.

The curvature of the shock wave BC makes the flow rotational in the central region of the wing. It was shown in (2) that on the lower surface the root chord is the line of convergence of the isentropic surfaces, whose equation is of the form

$$\left(\frac{d\xi}{d\eta}\right)_{\tilde{s}=\text{const}} = \frac{w - u\xi}{u\eta - v} \tag{16}$$

Then the lines of equal entropy in the (η,ξ) plane must be of the form shown schematically in Fig. 3. Since the shock AB is rectilinear, it is clear that the flow will be isentropic not only in the uniform flow region ABD but also in the region BDO which is subject to the influence of the apex of the wing. The position of the curve BO, which separates the rotational and irrotational portions of the flow, is unknown and must be determined.

Thus, the boundary-value problem for the region of influence of the apex of the wing on the side of the lower surface is stated in the following manner:

It is required to find the flow, that is, solve a system of differential equations (1) in the region $DBCO$, having uniquely determined the shape of the boundary of the region on the segment BC, for the following boundary conditions.

On the surface of the wing (OD) $\zeta = 0$:

$$w = 0 \qquad \tilde{s} = \tilde{s}_1 = \text{const}$$

In the plane of symmetry (OC) $\eta = 0$:

$$v = 0 \qquad \tilde{s} = \tilde{s}_2 = \text{const} \tag{17}$$

On the Mach cone BD:

$$\tilde{s} = \tilde{s}_1 = \text{const} \qquad w = 0$$

and u and v are determined from Eq. (8).

On BC Eqs. (14) are satisfied.

In the region BOD:

$$\tilde{s} = \tilde{s}_1 = \text{const}$$

Here $\tilde{s}_1$ is determined by (9) and $\tilde{s}_2$ by the shape of BC.

It should be noted that (3) stated the hypothesis that the boundary of the central region between the point B and the wing surface may be not the Mach cone BD but some shock wave starting at point B. We shall demonstrate that the calculations made in the present study did not support this hypothesis.

2. Method of Calculation and Results

Reference (2) proposed a method of solving the problem of flow past the lower surface of a delta wing. This method solves the problem, as a first approximation, on the assumption that the flow is isentropic on the side of the lower surface. The solution is then made more precise by taking entropy changes into consideration. Calculations made on a high-speed computer during the present investigation indicated that for large angles of attack and large Mach numbers ($\alpha > 5°$, $M > 3$), when the entropy change in the stream is considerable, it is practically impossible to obtain a first approximation, and hence to solve the problem, by the method proposed in (2).

In the present study the problem is solved by the method of successive corrections to the shape of the shock wave, resembling the method used in (1) to solve the problem of flow past the upper wing surface.

Let some shape BC for the shock wave be known. By specifying the shape of BC we define the values of u, v, w, and $\tilde{s}$ on it. If we require system (1) to be satisfied at the points of the jump BC, we thereby define the values of the derivatives of u, v, w, and $\tilde{s}$ along the normal to the shock wave. To solve system (1) within the region $CBDO$ it is sufficient to know the values of the desired functions on BC. Thus, at the jump BC the boundary conditions are overdefined. We make use of this fact to determine the shape of the shock wave BC. For some initially specified shape BC, using the values of the desired functions on BC, we apply grid and steepest-descent methods to find the solution of system (1) in the region $CBDO$. We then find the shape of the jump BC more precisely in such a way that the normal derivatives of the desired functions at the jump will assume the same values as are obtained by the solution within the region. After this we again solve system (1) and refine the shape BC still further. The process is continued until the last two shapes for the jump BC are identical.

In order to solve the problem by this method, we must have some initially specified shape of the density jump BC and some system of values of u, v, w, and s within $CBDO$, which will constitute the zeroth solution. The initial shape of the shock wave is given by

$$\xi = \xi_B + \frac{\eta_B}{1+m} \sin\chi \tan(\epsilon - \alpha_1) \left[1 - \left(\frac{\eta}{\eta_B}\right)^{1+m}\right] \quad (18)$$

The position of point C is determined by the value of m:

$$\xi_C = \xi_B + \frac{\eta_B}{1+m} \sin\chi \tan(\epsilon - \alpha_1)$$

This equation satisfies condition (15) and has certain advantages for the choice and study of different initial shapes of the jump: We can vary the shape BC simply by changing the value of the constant m.

System (1) is solved by a grid method. For this purpose region $CBDO$ is covered by a rectangular grid. The values of the grid intervals (h in η and l in ξ) are determined by

$$h = \frac{\eta_B}{E[k_1(\eta_B/\eta_D)]} \qquad l = \frac{\xi_B}{E[k_2(\xi_B/\xi_C)]}$$

Here $E(a)$ represents the integral part of a. By such a choice of the interval we can make sure that the known point B will always coincide with a node of the grid, which will simplify a number of arithmetic operations in the vicinity of point B. The values k_1 and k_2 indicate the number of grid nodes in the intervals OD and OC (to within ± 1). The values of k_1 and k_2 in our calculations were limited to 15 by the memory capacity of our computer.

In order to solve system (1) by the grid method, we replaced it by its finite-difference equivalent; all the partial derivatives appearing in the system were replaced by first central differences, so that, for example, for point (i,k) with $\eta = ih$, $\xi = kl$, we have

$$(\partial f/\partial \eta)_{ik} = (1/2h)(f_{i+1,k} - f_{i-1,k})$$
$$(\partial f/\partial \xi)_{ik} = (1/2l)(f_{i,k+1} - f_{i,k-1}) \quad (19)$$

Then system (1), after some minor transformations, becomes

$$v_{ik}(u_{i+1,k} - u_{i-1,k}) + \eta v_{ik}(v_{i+1,k} - v_{i-1,k}) + \eta w_{ik}(w_{i+1,k} - w_{i-1,k}) + \eta a_{ik}^2(\tilde{s}_{i+1,k} - \tilde{s}_{i-1,k}) + \frac{h}{l}[w_{ik}(u_{i,k+1} - u_{i,k-1}) + \xi v_{ik}(v_{i,k+1} - v_{i,k-1}) + \xi w_{ik}(w_{i,k+1} - w_{i,k-1}) + \xi \tilde{a}_{ik}^2(\tilde{s}_{i,k+1} - \tilde{s}_{i,k-1})] \equiv A_{ik} = 0$$

$$\eta u_{ik}(v_{i+1,k} - v_{i-1,k}) + u_{ik}(u_{i+1,k} - u_{i-1,k}) + w_{ik}(w_{i+1,k} - w_{i-1,k}) + \tilde{a}_{ik}^2(\tilde{s}_{i+1,k} - \tilde{s}_{i-1,k}) - \frac{h}{l}(w_{ik} - \xi u_{ik})(v_{1,k+1} - v_{i,k-1}) \equiv B_{ik} = 0 \quad (20)$$

$$(v_{ik} - \eta u_{ik})(w_{i+1,k} - w_{i-1,k}) - \frac{h}{l}[\xi u_{ik}(w_{i,k+1} - w_{i,k-1}) + u_{ik}(u_{i,k+1} - u_{i,k-1}) + v_{ik}(v_{i,k+1} - v_{i,k-1}) + \tilde{a}_{ik}^2(\tilde{s}_{i,k+1} - \tilde{s}_{i,k-1})] \equiv C_{ik} = 0$$

$$[\eta \tilde{a}_{ik}^2 + u_{ik}(v_{ik} - \eta u_{ik})](u_{i+1,k} - u_{i-1,k}) - [\tilde{a}_{ik}^2 - v_{ik}(v_{ik} - \eta u_{ik})] \times (v_{i+1,k} - v_{i-1,k}) + w_{ik}(v_{ik} - \eta u_{ik})(w_{i+1,k} - w_{i-1,k}) + \frac{h}{l}\{[\xi \tilde{a}_{ik}^2 + u_{ik}(w_{ik} - \xi u_{ik})](u_{i,k+1} - u_{i,k-1}) - [\tilde{a}_{ik}^2 - w_{ik}(w_{ik} - \xi u_{ik})](w_{i,k+1} - w_{i,k-1}) + v_{ik}(w_{ik} - \xi u_{ik})(v_{i,k+1} - v_{i,k-1})\} \equiv D_{ik} = 0$$

If we write system (20) for all N nodes of the grid, we obtain a system of $4N$ cubic equations in $4N$ unknowns u_{ik}, v_{ik}, w_{ik}, $\tilde{s}_{ik}$. (For brevity we shall call this the $4N$ system.) The $4N$ system is solved by the method of steepest descent. For this purpose we set up the following quadratic form for the $4N$ system:

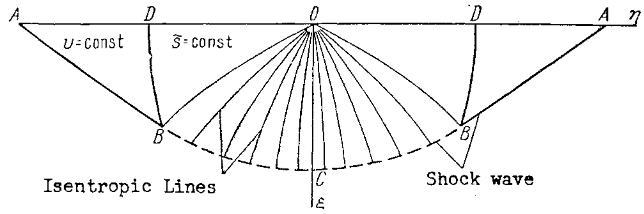

Fig. 3 Diagram showing supersonic flow past the lower surface of a delta wing (cross section perpendicular to the root chord).

$$\Phi = \sum_{i,k}^{4N} (A_{ik}^2 + B_{ik}^2 + C_{ik}^2 + D_{ik}^2) \quad (21)$$

The values of u, v, w, and $\tilde{s}$ corresponding to the zero minimum of Φ are the solutions of the $4N$ system. It should be noted that in changing from system (1) to the $4N$ system we are permitting a certain amount of error caused by replacing the derivatives by their finite-difference expressions. For this reason function Φ may not have a strict zero minimum. In that case the solution of system (1) will correspond to $\Phi_{\min} \neq 0$.

After replacing the boundary of the region $DBCO$ by the corresponding grid boundary, we calculate the initial value of the unknown functions for all the internal and boundary nodes of the resulting grid region. The zeroth values of u, v, and w are given by the following equations:

$$u = u_{00} - u_D\left(\frac{\eta}{\eta_D}\right)^m - \left[u_{00} - u_D\left(\frac{\eta}{\eta_D}\right)^m - u(\xi_i)\right]\left(\frac{\xi}{\xi_i}\right)^2$$

$$v = v_D\left(\frac{\eta}{\eta_D}\right)^m - \left[v_D\left(\frac{\eta}{\eta_D}\right)^m - v(\xi_i)\right]\left(\frac{\xi}{\xi_i}\right)^2 \quad (22)$$

$$w = w(\xi_i)\left(\frac{\xi}{\xi_i}\right)^2$$

Here u_D and v_D are the velocity components on AD, defined in accordance with (8); ξ_i are the values of ξ on BC at the points with $\eta = ih$, and u_{00} is the value of u at point 0.

The values of $u(\xi_i)$, $v(\xi_i)$ and $w(\xi_i)$ on BC were calculated from (14). In our calculations the value of m was taken equal either to 2 or to 3. Formulas (22) are satisfied by all the boundary conditions of (17). From certain general considerations we may expect that expansion flow will take place on OD. For this reason the value of u_{00} was chosen so as to produce a pressure drop between points D and O. Moreover, by Eq. (16), an isentropic line BO is formed, beginning at point B and separating the rotational and irrotational portions (BOC and BOD) of the central region. We noted in the foregoing that the isentropic lines must pass through point O. Since interval h was sufficiently small, the line BO, constructed in accordance with Eq. (16), invariably passed through point O, to a high degree of accuracy, in all the cases considered when the zeroth solution was given by Eq. (22), as well as for all successive approximations to be discussed.

In solving the problem we determined not the value s but the difference $s = \tilde{s} - \tilde{s}_1$, where $\tilde{s}_1$ is the value of $\tilde{s}$ behind the shock AB. Then $\tilde{s} = 0$ in the region ABO. In order to calculate the values of $\tilde{s}$ corresponding to the zeroth solution in the region BOC, the initial shapes of the isentropic lines were taken, for simplicity, to be those of straight lines passing through point 0. Then at each point (i,k) of the region BOC the value of s is equal to its value on the shock wave BC at its point of intersection with the straight line passing

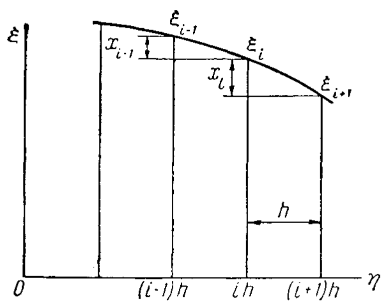

Fig. 4 Refining the shape of the pressure jump.

through points (i,k) and O. It is clear that this is strictly true only for points lying on OC.

Equation (21) may be considered as the equation of a hypersurface Φ in $(4N + 1)$ − dimensional space. The given zeroth solution defines some point on this surface. The minimum of Φ can be approached most rapidly in the direction opposite to that of grad Φ. For this purpose all the unknown functions must be replaced, in accordance with

$$\begin{aligned} u_{ik}^{(n+1)} &= u_{ik}^{(n)} - \lambda[\partial\Phi/\partial u_{ik}^{(n)}] \\ v_{ik}^{(n+1)} &= v_{ik}^{(n)} - \lambda[\partial\Phi/\partial v_{ik}^{(n)}] \\ w_{ik}^{(n+1)} &= w_{ik}^{(n)} - \lambda[\partial\Phi/\partial w_{ik}^{(n)}] \\ s_{ik}^{(n+1)} &= s_{ik}^{(n)} - \lambda[\partial\Phi/\partial s_{ik}^{(n)}] \end{aligned} \tag{23}$$

Here the indices n, $n + 1$, . . . represent the number of the approximation, and $\lambda = \text{const} > 0$. In determining the derivatives $\partial\Phi/\partial u_{ik}^{(n)}$, . . . it must be taken into account that quantities u_{ik}^{n}, . . . appear not only in the equations

$$A = B = C = D = O$$

written for point (i, k) but also in the equations written for the neighboring nodes of the grid; for example, the quantity u_{ik}^{n} appears not only in the equations

$$A_{ik} = B_{ik} = C_{ik} = D_{ik} = O$$

but also in the equations

$$\begin{aligned} A_{i+1,k} = B_{i+1,k} = D_{i+1,k} &= O \text{ in the form } u_{i-1,k} \\ A_{i-1,k} = B_{i-1,k} = D_{i-1,k} &= O \text{ in the form } u_{i+1,k} \\ A_{i,k+1} = C_{i,k+1} = S_{i,k+1} &= O \text{ in the form } u_{i,k-1} \\ A_{i,k-1} = C_{i,k-1} = D_{i,k-1} &= O \text{ in the form } u_{i,k+1} \end{aligned}$$

Before substituting values into Eqs. (23) we must calculate the value $\lambda = \lambda_{\min}$ corresponding to the minimum of the function

$$\Phi_n = \Phi_n\left(u_{ik}^{(n)} - \lambda\frac{\partial\Phi}{\partial u_{ik}^{(n)}}, \ldots\right) = \Phi_n(\lambda) \tag{24}$$

In order to substitute the value of $\lambda_{\min}$, beginning at $\lambda = 0$, for the values of λ, increasing at some interval Δ, we calculate the values of $\Phi_n(\lambda)$. The calculation is continued until we obtain $\partial\Phi/\partial\lambda \geq 0$. Then by refining the interval Δ we find the value $\lambda_{\min}$ (to an arbitrarily specified degree of accuracy). From the value of $\lambda_{\min}$, using formulas (23), we calculate the next approximation. The calculation of the approximations is continued until we obtain the nth approximation, for which the rate of decrease of $\Phi_n(\lambda_{\min})$ as n increases becomes negligible:

$$\left|\frac{\Phi_n(\lambda_{\min n})}{\Phi_{n-1}(\lambda_{\min, n-1})} - 1\right| < \delta \tag{25}$$

In our calculations the value of Δ was taken equal to 0.01. The value of $\Phi_n(\lambda)$ varied from 0.00001 to 0.0001.

It was shown in (3) that the line BO separating the rotational and irrotational portions of the flow is a singular line. To see this, we note that, since $s \equiv 0$ in the region BDO and $s \not\equiv 0$ in the region BCO, it follows that upon crossing BO the normal derivatives (first or higher) of s must necessarily be discontinuous. Then, from the equations of motion, it follows that similar discontinuities will occur in the normal derivatives of u, v, and w as well. For that reason, when we calculated the derivatives of the velocities and of the entropy function we always used values of u, v, w, and s at points lying on only one side of the line BO. As a result, formulas (19) became unsuitable for use in the case of points lying near the line BO and were replaced by the corresponding one-sided difference formulas.

We speeded up the computing process by calculating the new position of BO after each approximation was determined and correcting the boundary values of the velocities and the entropy at the boundary points of the grid by using linear interpolation (or extrapolation) between the points of the jump BC and the nearest interior nodes of the grid.

After finding the solution for a given shape of the shock wave BC, we make an appropriate correction in that shape.

Let $f = f(\eta)$ be the equation of the shock wave. If the arc length along the jump is represented by σ, then for an arbitrary quantity ψ we have

$$\frac{d\psi}{d\sigma} = \frac{\partial\psi}{\partial\eta}\cdot\frac{d\eta}{d\sigma} + \frac{\partial\psi}{\partial\xi}\cdot\frac{d\xi}{d\sigma}$$

Hence

$$\frac{\partial\psi}{\partial\eta} = \sqrt{1 + f'^2}\cdot\frac{d\psi}{d\sigma} - \frac{\partial\psi}{\partial\xi}\cdot f' \tag{26}$$

For the sake of brevity we introduce the notation

$$\sqrt{1 + f'^2}\,\frac{d\psi}{d\sigma} = A_\psi$$

Writing Eq. (26) for all velocities and the entropy, substituting into the equations of motion, and solving them for the derivatives with respect to ξ, we obtain

$$\begin{aligned} \frac{\partial w}{d\xi} &= \frac{1}{(\omega_1^2 - \tilde{a}^2\omega_2)\omega_1}[\omega_1 B_1 - (\tilde{a}^2 f' - v\omega_1)(B_2 + f'B_3) - \\ &\qquad (\tilde{a}^2 q - u\omega_1)(B_3 q - B_1)] \\ \frac{\partial u}{\partial\xi} &= \frac{1}{\omega_1}(B_3 q - B_1) - q\cdot\frac{\partial w}{\partial\xi} \\ \frac{\partial v}{\partial\xi} &= \frac{1}{\omega_1}(B_2 + f'B_3) - f'\cdot\frac{\partial w}{\partial\xi} \\ \frac{\partial S}{\partial\xi} &= \frac{v - u\eta}{\omega_1}\cdot A_s \end{aligned} \tag{27}$$

Here ω_1 and ω_2 are calculated from the velocity values behind the shock wave:

$$\begin{aligned} q &= \xi - f'\eta \\ B_1 &= -(vA_u + v\eta A_v + \omega\eta A_w + \tilde{a}^2\eta A_s) \\ B_2 &= -(uA_u + u\eta A_v + wA_w + \tilde{a}^2 A_s) \\ B_3 &= (v - u\eta)A_w \\ B_4 &= -\{[\tilde{a}^2\eta + u(v - u\eta)]A_u - \\ &\qquad [\tilde{a}^2 - v(v - u\eta)]A_v + w(v - u\eta)A_w\} \end{aligned}$$

If the system of values of u, v, w, and s defined in the region $CBDO$ is a solution of system (1) and the shape of the shock BC corresponds to its true position, then on BC the values of the normal derivatives of the desired functions determined from the shape of the shock wave must agree with those obtained by using the solution within the region. Instead of the normal derivatives we may consider derivatives in any direction other than the tangent. For simplicity of computation, we shall consider the derivatives along ξ. Then we can refine the shape of the shock wave by using the equations

$$\frac{\partial u}{\partial \xi} = \left(\frac{\partial u}{\partial \xi}\right)_{\text{int}} \qquad \frac{\partial v}{\partial \xi} = \left(\frac{\partial v}{\partial \xi}\right)_{\text{int}}$$
$$\frac{\partial w}{\partial \xi} = \left(\frac{\partial w}{\partial \xi}\right)_{\text{int}} \qquad \frac{\partial s}{\partial \xi} = \left(\frac{\partial s}{\partial \xi}\right)_{\text{int}} \tag{28}$$

Here the derivatives with respect to ξ which have the subscript "int" are determined from the solution in the interior of the region *CBDO* by numerical differentiation. We substitute the expressions of (27) into the left-hand parts of Eqs. (28), so that system (28) is replaced by

$$\left(\frac{\partial u}{\partial \xi} - \frac{\partial u}{\partial \xi_{\text{int}}}\right)^2 + \left(\frac{\partial v}{\partial \xi} - \frac{\partial v}{\partial \xi_{\text{int}}}\right)^2 + \left(\frac{\partial w}{\partial \xi} - \frac{\partial w}{\partial \xi_{\text{int}}}\right)^2 + \left(\frac{\partial s}{\partial \xi} - \frac{\partial s}{\partial \xi_{\text{int}}}\right)^2 = 0 \tag{29}$$

We refine the shape of the shock *BC*, starting from the known point *B* in the direction of the plane of symmetry of the flow *OC*. At each point of the shock wave for which $\eta = ih$ we have (see Fig. 4):

$$\xi i = \xi_{i+1} + x_1 \qquad f_i' = -(x_i/h) \tag{30}$$

Substituting (30) into (29), for a known ξ_{i+1} we obtain an equation for finding x_i. Since the calculation is approximate, it may happen that there is no value of x_i for which Eq. (29) is strictly satisfied. Therefore in our calculations a method similar to that used for finding $\lambda_{\min}$ was used to determine the value of x_i for which the left-hand member of Eq. (29) became a minimum. The condition $0 \leq x_i \leq x_{i+1}$ also must be satisfied, that is, the shock wave from *B* to *C* must decrease. After determining the new shape of the shock wave, we constructed the grid boundary along *BC*, and linear interpolation (or extrapolation) between the points of *BC* and the nearest interior nodes of the grid was used to transfer the boundary values of the desired functions to the grid boundary. If, after the shape of *BC* has been refined, new interior nodes appear in the region *CBDO*, then we calculate the values of the desired functions for those points, again by interpolation. After this, we again solve system (27) for the new shape of the region *CBDO* and again refine the shape of *BC*. The process is continued until the last two shapes for the shock wave *BC* agree (to some given degree of accuracy). The calculations show that when a solution is obtained by this method, the various shapes of the shock

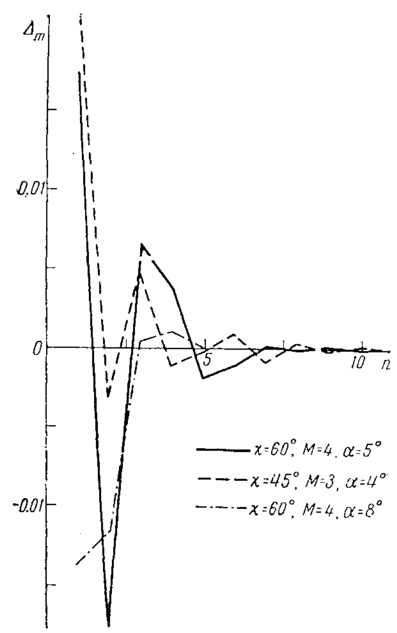

Fig. 5.

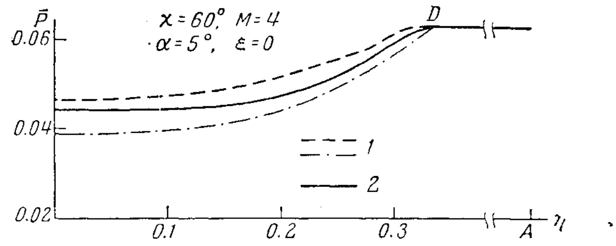

Fig. 6 1) Initial solution; 2) final solution.

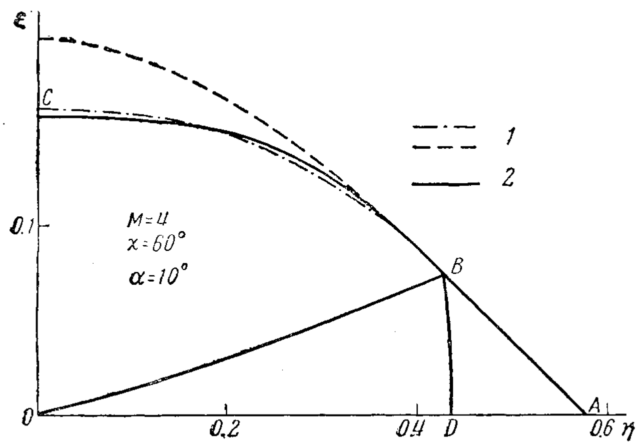

Fig. 7 1) Initial shapes of shock; 2) final solution.

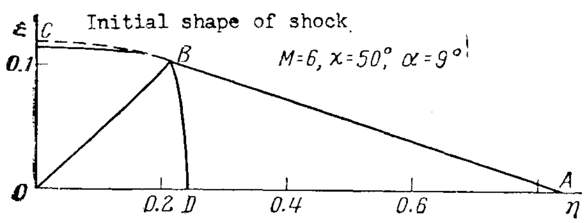

Fig. 8.

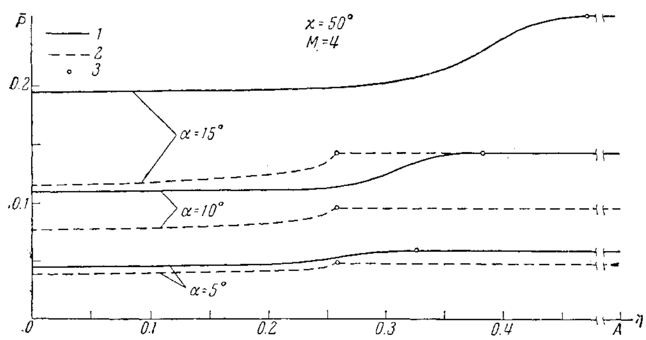

Fig. 9 1) Numerical solution; 2) linear theory; 3) boundary of central region.

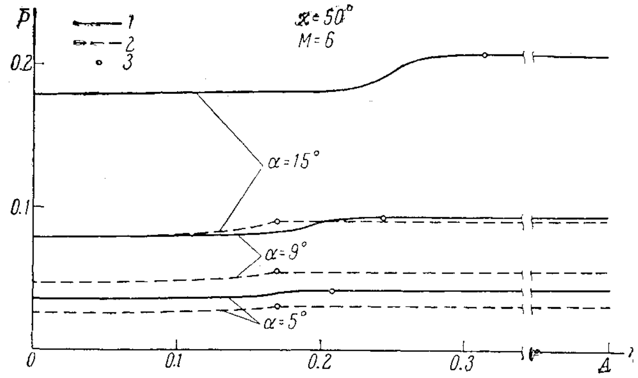

Fig. 10 1) Numerical solution; 2) linear theory; 3 boundary of central region.

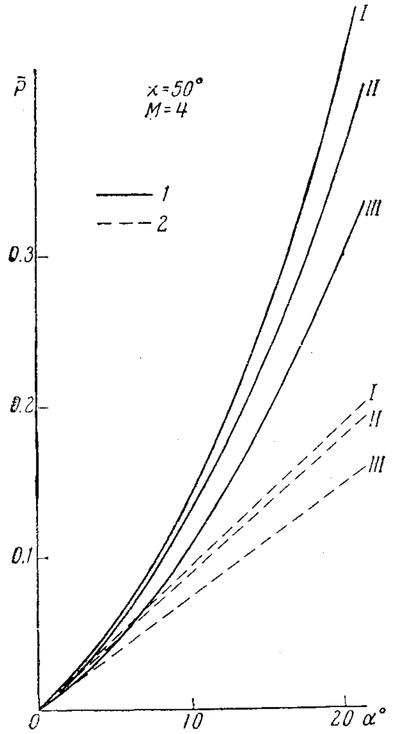

Fig. 11 1) Numerical solution; 2) linear theory; I) $\bar{P}$ on *AD*; II) C_{nl}; III) $\bar{P}$ on root chord.

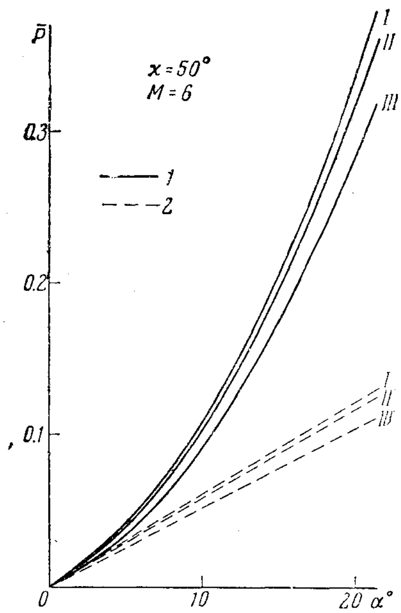

Fig. 12 1) Numerical solution; 2) linear theory; I) $\bar{P}$ on *AD*; II) C_{nl}; III) $\bar{P}$ on root chord.

wave oscillate about the true shape, gradually approaching it as the number of approximations increases. Figure 5 shows, for a number of cases, the variation in the maximum distance (in absolute value) along the ξ axis between two successive shapes of the shock wave

$$\Delta_m = \text{sign}(\xi_{in} - \xi_{i,n-1}) \max|\xi_{in} - \xi_{i,n-1}| \quad (0 \leqslant i \leqslant i_B)$$

as a function of the number n of approximations. It can be seen for $n = 11$, $|\Delta_m| < 10^{-4}$.

It should be noted that if system (20) is solved by the method of steepest descent, we may obtain, in general, not an absolute minimum of function Φ, which would correspond to the true solution, but some relative minimum. In order to clarify this, we specified different zeroth solutions and different initial shapes of the density jump for the same case. This corresponds to different initial points on the hypersurface Φ. In all the cases we checked, regardless of the shape of the zeroth solution and the initial shape of the shock wave *BC*, the calculation produced the same result (when P was on the wing surface to an accuracy of 1% and the position of the shock waves was specified to the third decimal place), which may be taken as an indication that the true solution was obtained. Figures 6 and 7 show examples of such checks, indicating the distribution of the pressure coefficient along the wing surface and the shape of the density jump *BC*. Here the solid curves correspond to the results we obtained, and the other curves to the various initial solutions.

Reference (4) stated the hypothesis that a shock wave could occur in the vicinity of the Mach cone *BD*. As has been indicated, on the true boundary of the region the resulting solution must insure agreement not only between the boundary values of the desired functions themselves but also between their normal derivatives. Using this condition, after finding the solution, as was done in refining the shape of the shock *BC*, we determined the shape of the boundary of the central region between point *B* and the wing surface. The derivatives with respect to ξ in Eq. (29) were replaced by derivatives with respect to η, and the boundary of the region was constructed from the point *B* downward to the wing surface. In all the cases we checked, the boundary obtained in this manner coincided with the Mach cone *BD*, which is a shock wave of zero magnitude. Thus we showed that there is no shock wave between point *B* and the wing surface.

Figures 7 and 8 show, for a number of cases, the flow past the lower wing surface obtained by calculation. Figures 9 and 10 show the calculated pressure distribution on the lower wing surface. It can be seen that the numerical solution differs considerably from the data of the linear theory; as the angle of attack and the Mach number increase, this difference becomes greater. This can also be seen from Figs. 11 and 12, which show the values of the pressure coefficient near the leading edge in the region of uniform flow (on *AD* in Fig. 3) and on the root chord, as well as the normal force coefficient for the lower wing surface, C_{nl}.

According to the linear theory the boundary of the central region is defined by the Mach number

$$\eta_D = \frac{1}{\sqrt{M^2 - 1}}$$

and does not depend on the angle of attack or on the sweepback angle χ. The exact value of η is found from the formula

$$\eta_D = \frac{uv - \sqrt{Q(U^2 - Q)}}{Q - v^2}$$

where u and v are calculated from (8).

As the sweepback angle χ and the angle of attack α increase, the dimensions of the central region also increase.

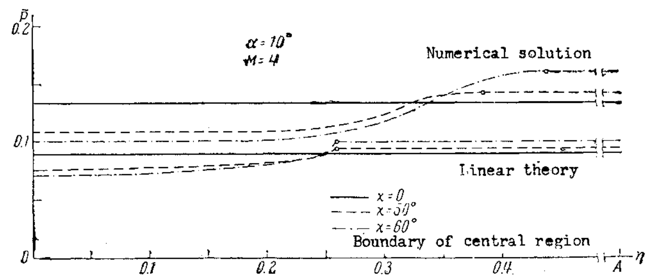

Fig. 13.

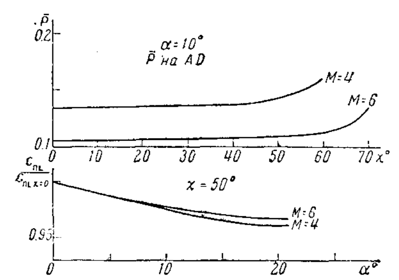

Fig. 14.

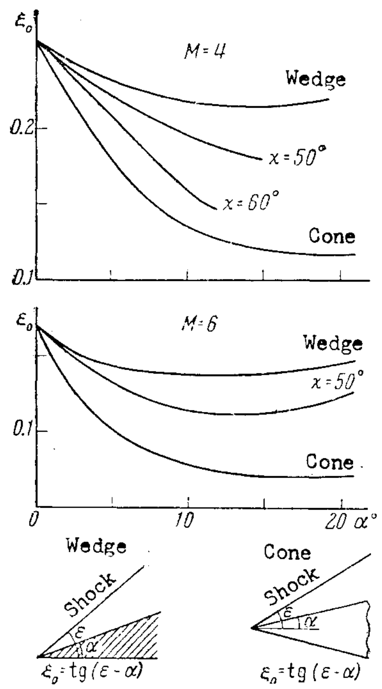

Fig. 15.

This can be seen from Figs. 9, 10, and 13. According to the linear theory, as the sweepback angle of the delta wing increases, the pressure will increase near the leading edge but will decrease at the root chord (Fig. 13). This qualitative pressure relationship is confirmed by the exact calculations (Figs. 13 and 14). As a result of the previously indicated pressure variation, the lift force of the delta wing, within the limits of the linear theory, is independent of the sweepback angle and is equal to its value corresponding to a wing of infinite spread ($\chi = 0$). The calculations show that when the problem is solved exactly, the normal force on the lower wing surface still varies only slightly with the sweepback angle χ. Thus for $M = 4$–6 and $\alpha \leq 21°$ a variation in χ from 0 to 50° produces a decrease of only 3–4% in C_{ml} (Fig. 14). This conclusion is also valid for the upper wing surface. For the cases discussed in (1) ($M = 4$–6, $\alpha \leq 7°$), an increase in χ from 0 to 60° produces a decrease of no more than 2.5% in the coefficient of normal force on the upper wing surface. Thus, for the cases of independent flow past the two surfaces, the coefficient of normal force on a plane delta wing may be considered equal to the coefficient of normal force on an infinite plate, with an accuracy sufficient for many practical purposes.

In the plane of symmetry of the wing the shock wave on the side of the lower wing surface assumes a position intermediate to the shocks due to the corresponding circular cone and wedge. As the sweepback angle increases, the shock wave is displaced toward the position corresponding to the circular cone (Fig. 15).

—Submitted March 15, 1962

References

[1] Babaev, D. A., "Numerical solution of the problem of supersonic flow past the upper surface of a delta wing," Zhur. Vychislitel'noi Matematiki i Matematicheskoi Fiziki (J. Computational Math. and Mathemat. Phys.) 2, No. 2, 278–289 (1962).

[2] Fowell, L. R., "Exact and approximate solutions for the supersonic delta wing," J. Aeronaut. Sci. 8, 709–720 (1956).

[3] Bulakh, B. M., "Comments on the paper by A. Ferri, 'Recent theoretical work in supersonic aerodynamics at the Polytechnic Institute of Brooklyn'," Prikl. Mat. i Mekhan. (Appl. Math. and Mech.) 23, No. 3, 576–580 (1959).

[4] Bulakh, B. M., "On the theory of nonlinear conical flows," Prikl. Mat. i Mekhan. (Appl. Math. and Mech.) 19, No. 4, 393–409 (1955).

Reviewer's Comment

This is an interesting and significant paper, both from the gasdynamical and computational point of view. Since the author's solution for the upper side was published in the USSR just prior to this paper, it appears that we finally have an exact numerical solution for the delta wing with supersonic edges to place in our tiny collection of exact solutions to the gasdynamic equations in three dimensions. Numerical attempts at this problem and other such conical flows have appeared sporadically for about fifteen years. Some strong criticism has been leveled in the process. The last such critic and extender, Bulakh, comes in for some criticism himself in this paper.

The field equations used in the formulation are conventional (Crocco equations plus the flow equation). The numerical method used (successive solution of nonlinear central difference equations by steepest descent from zeroth solution) is about as simple as one could reasonably ask for. Probably the main contribution, however, is the verification of the wave configuration. The explanation is clear, detailed, and thorough enough. The method depends (probably unavoidably) on choosing a suitable zeroth approximation. The choice made appears to be simple but shrewd. For higher Mach numbers and angles of attack, an isentropic zeroth solution (such as the linearized solution with the levels adjusted; this solution has all of the qualitative trends) does not seem to yield convergence. Other workers have encountered the same difficulty subsequent to its proposal by Fowell. Some initial provision for entropy variation must be made. Within the class of zeroth solutions used, the author demonstrates convergence for quite different initial choices. In the case of other conical flows, one would presumably be hard pressed for a choice of a zeroth solution. The singularities and qualitative behavior of exact, isentropic (limit surfaces in place of shocks), conical flows have recently been studied exhaustively by Reyn.[1] It appears that this work would unfortunately have to be augmented by entropy consideration to arrive at a suitable zeroth approximation.

The worker who wishes to have a solution to the flat plate delta wing for other sets of parameters (stream Mach number, sweep angle angle of attack, and specific heat ratio) still has a formidable task before him. Since there are two independent variables, tables like Z. Kopal's cone tables would not seem to provide the answer either. Perhaps the practical solution would be to do what D. B. Spalding has done so elaborately for the results of boundary layer calculations, i.e., to undertake the extensive curve fitting of machine solutions. A fully analytic uniform solution, to second order in incidence, of the same delta wing problem was recently presented by Clarke and Wallace.[2] The two types of solutions appear to complement each other nicely.

The author's conclusion that the normal force is virtually independent of sweep angle, and can be computed from two-dimensional theory, is very interesting indeed. The independence can be proved up to second order in incidence. But it can also be shown to second order that the conclusion is modified by the presence of wing thickness because of a second-order thickness-incidence coupling effect.

—Joseph H. Clarke
Division of Engineering
Brown University

[1] Reyn, J. W., Arch. Ratl. Mech. Anal. 6, 299–354 (1960).

[2] Clarke, J. H. and Wallace, J., Div. Eng. Rept. CM-1034, Brown University, Providence, R. I. (April 1963).